Multiple Melting and Partial Miscibility of Ethylene-Vinyl Acetate Copolymer/Low Density Polyethylene Blends

Xuming Shi, Jing Jin, Shuangjun Chen, Jun Zhang

College of Materials Science and Engineering, Nanjing University of Technology, Nanjing 210009, People's Republic of China

Received 10 June 2008; accepted 17 February 2009
DOI 10.1002/app.30271
Published online 1 May 2009 in Wiley InterScience (www.interscience.wiley.com).

ABSTRACT: Multiple melting behaviors and partial miscibility of ethylene-vinyl acetate (EVA) copolymer/low density polyethylene (LDPE) binary blend via isothermal crystallization are investigated by differential scanning calorimetry (DSC) and wide angle X-ray diffraction (WAXD). Crystallization temperature T (°C) is designed as 30, 50, 70, 80°C with different crystallization times t (min) of 10, 30, 60, 300, 600 min. The increase of crystallization temperature and time can facilitate the growth in lateral crystal size, and also the shift of melting peak, which means the completion of defective secondary crystallization. For blends of various fractions, sequence distribution of ethylene segments results in complex multiple melting behaviors during isothermal crystallization process. Overlapping endothermic peaks and drops of equilibrium melting points of LDPE component extrapolated from Hoffman–Weeks plots clarify the existence of partial miscibility in crystalline region between EVA and LDPE. WAXD results show that variables have no perceptible influence on the predominant existence of orthorhombic crystalline phase structure. © 2009 Wiley Periodicals, Inc. J Appl Polym Sci 113: 2863–2871, 2009

Key words: EVA; LDPE; partial miscibility; multiple melting; blend; crystalllization; differential scanning calorimetry (DSC); polyolefins; wide angle x-ray diffraction (WAXD)

INTRODUCTION

Ethylene-vinyl acetate (EVA) copolymer is a kind of typical thermoplastic semi-crystalline ethylene copolymer. For its special molecular configuration and excellent characteristics, EVA is commonly used as modifier to other raw resins for property optimization. As one of the most widely used commercial polymeric materials, low density polyethylene (LDPE) owns excellent properties, moderate cost, and good compatibility.[1–3] Blending LDPE with EVA could modify LDPE fracture toughness, processibility. It is an economical and efficient alternative to the development of new polymers. The introduction of polar ester groups into the blends can also provide better miscibility with inorganic fillers. Mixing of crystalline with semi-crystalline polymers gives rise to a huge potential in tailoring desirable properties in blends, also more complex crystallization mechanism. The complex crystallization behavior of blend is valuable for investigation.

Investigation of polymer crystallization behavior is necessary for improving manufacturing technique.[4–6] Multiple melting behaviors resulted from complex crystallization of unitary semi-crystalline polymer in isothermal crystallization possess considerable haninterests.[7,8] To EVA, this is proposed as some kind of chain segments fractionation classified by chain structure.[9] Researches in confined crystallization behavior of analogous binary, ternary blending systems, involving crystalline or semi-crystalline components have also been widely researched, such as in mLLDPE/LDPE,[10] EVA/PP/LLDPE,[11] and EVA/LLDPE[12] systems. Moly[13] proposed the hindrance to chain mobility of EVA affected the crystallization of another component in blend. Russell[14] and Uehara[15] have also discussed the co-existence and transitions between different crystal phases of polyethylene.

Miscibility is one of the most important properties characterizing the practical value of polymer blends. Khonakdar et al.[2] proposed the lower viscosity ratio and lower interfacial tension between components could lead to better miscibility and interconnected morphology in blends. The shift of melting peak temperature also indicates the miscibility in mixture, which involves both effects from morphological and thermodynamic factors. Paul,[16] Yoon[17,18] and Kundu[19] utilized Hoffman–Weeks equilibrium melting point to separate the morphological effect from thermodynamic effect in connecting the melting point depression behavior with miscibility characterization between components. Both immiscibility and partial miscibility of EVA/LLDPE systems have been discussed earlier.[12,13,20,21] LDPE with broader short chain

Correspondence to: J. Zhang (zhangjun@njut.edu.cn).

sequences distribution than LLDPE may lead to easier partial miscibility when it was blended with EVA.

The present study was to investigate the multiple melting behaviors and miscibility characterization in isothermal crystallization process of EVA/LDPE binary blend, which were analyzed in terms of component ratio, crystallization time and temperature. Hoffman–Weeks equilibrium melting point extrapolation was utilized for partial miscibility characterization. Influences on crystallinity from factors discussed above were also evaluated via differential scanning calorimetry (DSC) and wide angle X-ray diffraction (WAXD).

EXPERIMENTAL

Materials

EVA copolymer with 14 wt % VAc (EVA 14-2) was supplied by Beijing Organic Chemistry Plant, China; Low density polyethylene (LDPE 2426H) was obtained from BASF-YPC, China as received.

Preparation of samples

Twin-screws extruding

Blends of EVA and LDPE (mass ratio EVA/LDPE=3/7, 5/5, 7/3) were first mixed and granulated via twin-screw extruder (TE-20, Nanjing Keya Machinery, China) with effective length to diameter ratio (L/D) at 32. The extruder had three separate temperature-controlled barrel zones and one die zone, which were set as 120°C, 140°C, 150°C and 130°C, respectively. All blends were mixed at a screw speed of 180 rpm.

Injection molding

EVA/LDPE blends including virgin EVA and LDPE pellets were injected by small plunger injection molding machine (RR/TSMP. RAY-RAN Test Equipment, UK). The barrel temperature was set as 170°C for EVA, 215°C for LDPE and 190°C for EVA/LDPE blends. The mold temperature was maintained at 30°C with maximum injection pressure of 0.76 MPa (110 psi). Specimens of 2 mm thickness were prepared for DSC, and 0.5 mm slices were prepared for WAXD.

Isothermal crystallization process

In order to erase former thermal history, materials in small chamber mold under moderate pressure were first thoroughly melted at 135°C for 15 min. Subsequently, mold was immerged in circular water bath with stable temperature. Variable water temperature was assigned as T (°C) = 30, 50, 70, 80. Different crystallization time was designated as t (min) = 10, 30, 60, 300, 600. Finally, mold was quickly placed into ice water (0°C) for pausing crystallization process. Quenched materials were placed directly into ice water (0°C) for 5 min after having been thoroughly melted at 135°C for 15 minutes.

Characterization techniques

WAXD measurement

WAXD (Shimadzu XRD-6000, Japan) measurement was used to characterize the crystalline microscopic structure of polymer. The radiation source (CuKα X-ray) was operated at 40 kV, 30 mA. Scan was in 0.05° steps at speed of 4°/min. The scanning angle ranged from 5° to 45°. The Bragg equation was used to calculate the lattice distance (d_{hkl}), equation is given as[22]

$$d_{hkl} = \frac{\lambda}{2 \sin \theta_{hkl}} \tag{1}$$

where $\lambda = 1.541$ Å, θ_{hkl} represents the Bragg angle. The lateral crystal size (L_{hkl}) was calculated by Scherrer formula

$$L_{hkl} = \frac{K\lambda}{\beta_{hkl} \cos \theta_{hkl}} \tag{2}$$

where the structure factor $k = 1.0$, β_{hkl} is the peak width of half height of the crystal plane reflection. The crystallinity of sample can also be obtained from WAXD. The ratio of the area under the crystalline peaks to the entire area under the diffraction curve represents the crystallinity. In this work, Pseudo-viogt profile function[23] was used to separate the crystalline peaks from the amorphous halo and to fit the diffraction pattern. The overall crystallinity X_c was calculated by

$$X_c = \frac{I_c}{I_a + I_c} = \frac{\sum I_{\text{crystalline}}}{\sum I_{\text{amorphous}} + \sum I_{\text{crystalline}}} \times 100\% \tag{3}$$

$I_{\text{crystalline}}$ and $I_{\text{amorphous}}$ are the fitted crystalline and amorphous areas, respectively, crystallinity was determined with a residual error of fit less than 6%.

DSC analysis

Studies on the melting behavior of polymer were carried out via thermal analysis apparatus (Pyris 1 Perkin-Elmer DSC, USA) with appropriate sample (about 10 mg) sealed in aluminum pans. The heating rate was 10°C/min with the temperature range from 0°C to 150°C in a flowing argon atmosphere. The crystallinity X_c (%) was evaluated by[13]:

$$X_c = \frac{\Delta H_f}{\Delta H_f^*} \times 100\% \tag{4}$$

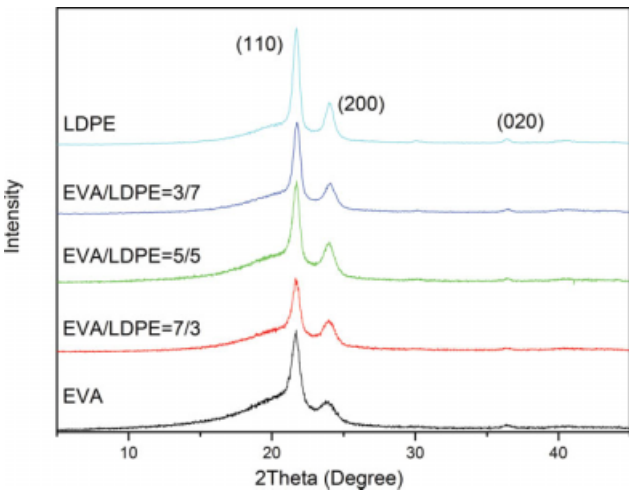

Figure 1 WAXD patterns of EVA/LDPE blends with various ratios isothermally crystallized at 80°C for 10 min. [Color figure can be viewed in the online issue, which is available at www.interscience.wiley.com.]

where the ΔH_f and ΔH_f^* (277.1 J/g)[24] represent the melting enthalpy of sample and 100% crystallized PE, respectively.

RESULTS AND DISCUSSION

Effect of EVA proportion

WAXD scan

Figure 1 presents the X-ray diffraction patterns of blends with different EVA population ratios, which were isothermally crystallized at 80°C for 10 min. Existence of monoclinic, orthorhombic crystal phase structure and their co-existence in crystallization of polyethylene have been reported.[25,26] The monoclinic/orthorhombic ratio in ethylene copolymer would increase with the co-monomer content increasing under cooling condition,[25] especially when co-monomer owns bulk side group. However, it is clear that, in addition to the amorphous halo, all patterns show typical orthorhombic crystal phase diffraction peaks at about 21.6°, 23.8°, and 36.3°, representing the (110), (200), and (020) crystal plane, respectively. The characteristic diffraction peaks of monoclinic phase at 19.5°, 23.2° and 25.1° of (001), (200), (-201) planes reported by Russell[14] are not perceptible in present work.

Diffraction data of correlative scanning are shown in Table I, along with the depressing EVA fraction in mixture, diffraction peaks of (110), (200) plane shift to higher position. Component ratio changing has no apparent influence on the position of (020) plane peak; this might result from the diffraction cacophony affection during scanning process. Based on the Bragg equation, *d-Val* of the former planes, which represents lattice distance (d_{hkl}) shows gradually shrinking tendency. This is in accordance with the former conclusion from Moly's research on non-isothermal crystallization behaviors of EVA/LLDPE system.[13] In this study, lattice distance shrinks as the increase of LLDPE content, in an even obvious trend, resulting from the incorporation of EVA chains in the LLDPE crystals. L_{hkl} of each plane in Table I is calculated from the β_{hkl} of each pattern via Scherrer formula. It reveals an apparent upward growing tendency of lateral crystal size[27,28] as the increase of LDPE in population. Ascending in crystal size implies the formation of more perfect crystalline structure. Analysis above clarifies the baffling effect of EVA in blends.

DSC analysis

The sequence length ξ of crystallizable units in the random co-polymer should be statically determined by the co-polymer chain. When the VAc content is so small in the molecule that the sequence length ξ of crystallizable units is larger than the thickness L_f of chain-folded crystal, the polymer could crystallize in the form of chain-folded lamellae.[9] As for those molecules with crystallizable unit shorter than the thickness L_f, chain segments will become unable to fold back on crystallization on its own. In that case the form of crystal is inter-molecular in nature, and it is anticipated that some of these molecular species can be crystallized into the bundle-like crystals form.[9] Li[20] also proposed that each melting peak in DSC traces represented the fusion of lamellae population formed by the linear chain segments of approximately similar short chain branching content, such chain segments' fractionation is sorted by crystallizable unit length. According to the kinetic

TABLE I
WAXD Data of Blends with Various Ratios Crystallized at 80°C for 10 min

Sample name	2θ (°)	Crystal plane	*d-Val* (Å)	L_{hkl} (Å)
Neat EVA 14-2	21.6	110	4.11	99.7
	23.8	200	3.73	69.0
	36.4	020	2.47	151.6
EVA/LDPE = 7/3	21.6	110	4.11	115.2
	23.9	200	3.72	82.0
	36.4	020	2.47	140.8
EVA/LDPE = 5/5	21.7	110	4.09	130.3
	23.9	200	3.72	95.0
	36.4	020	2.46	202.0
EVA/LDPE = 3/7	21.7	110	4.09	142.7
	24.1	200	3.70	98.1
	36.4	020	2.47	172.1
Neat LDPE	21.7	110	4.09	155.0
	24.0	200	3.71	123.6
	36.4	020	2.47	168.9

2θ, Bragg angle; *d-Val*, lattice distance; L_{hkl}, lateral crystal size.

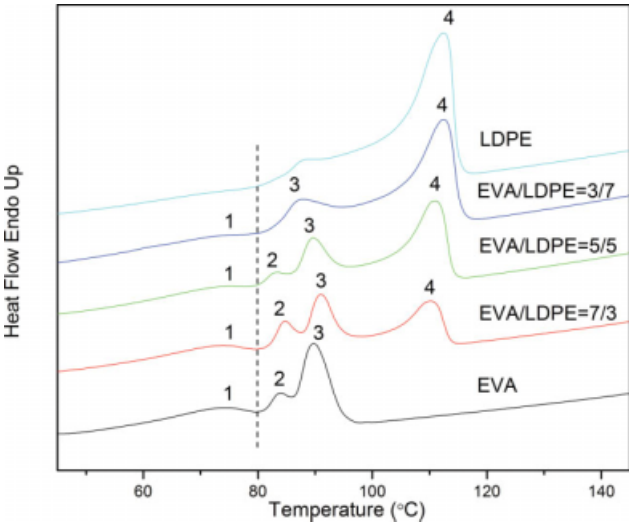

Figure 2 Endotherms of EVA/LDPE blends with various ratios isothermal crystallized at 80°C for 10 min. [Color figure can be viewed in the online issue, which is available at www.interscience.wiley.com.]

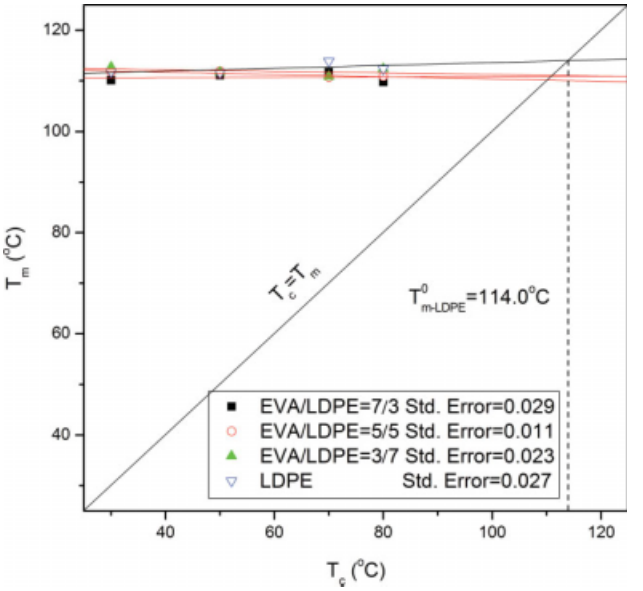

Figure 3 Hoffman–Weeks plots (T_m vs. T_c) of LDPE component in binary mixture. [Color figure can be viewed in the online issue, which is available at www.interscience.wiley.com.]

theory, the intra-molecular structure owns comparative smaller crystal thickness L_f than the bundle-like form. That means the chain-folded crystallization has more compact structure and is easier than the bundle-like crystallization.

The heating endotherms of LDPE and EVA along with their blends after isothermally crystallized at 80°C for 10 min were presented in Figure 2. Complex multiple melting behaviors were observed in EVA and its blends. As the predominant status of orthorhombic phase in samples has been validated above, it is clear that multiple melting could not be attributed to the various crystalline phases. The VAc content in EVA was 14% (wt), the majority of crystallizable linear ethylene chain segments were long enough to fold back and form intra-molecular crystallites in a comparative fast speed, which referred to the primary melting peak 3 in EVA. Polar VAc groups were considered to be randomly distributed along the backbone. These un-crystallizable units were excluded from the existing crystalline lattice, and affected the crystallizability of its adjacent ethylene chain segments. Defective chains were forced to concentrate at the amorphous–crystalline interface. This gave rise to a fringed micelles structure between the crystal and amorphous region. The lower melting peak 2 attributes to the inter-molecular crystallization with comparative defective bundle-like structure. Similar multiple melting in other semi-crystalline polymers, such as poly (ethylene terephthalate)[29,30] and poly (ferrocenyldimethylsilanes)[31] systems were widely debated, which were also designated as the secondary crystallization behavior. In Righetti, Cebe and Schick's recent works,[32–35] they also proposed that, the origin of such endotherm, a few degrees above the crystallization temperature (such as peak 2 in Fig. 3), were caused not only by melting of lamellae formed during secondary crystallization, but also could contain some contribution from the enthalpy recovery linked to mobilization of rigid amorphous fraction in polymer, or by both processes occurring simultaneously. Melting peak 1 is even lower than the crystallization water bath temperature. This may corresponds to the endotherm of the most defective crystal by shortest crystallizable units, which were failed to obtain enough mobility at 80°C but were only able to crystallize while being quenched in ice water (0°C), under the intense cooling condition.[9]

As is shown in Table II, in blend ratio at EVA/LDPE = 7/3, melting peak 3 of folded chain crystal shifts to a higher position. The bundle-like crystal peak 2 shows increasing in magnitude than in neat

TABLE II
Melting Peak Temperature of Blends Crystallized at 80°C for 10 min

Sample name	T_1	T_2	T_3	T_4
Neat EVA 14-2	74.5	84.1	89.8	–
EVA/LDPE = 7/3	73.9	86.2	91.4	109.8
EVA/LDPE = 5/5	73.2	83.3	89.7	110.9
EVA/LDPE = 3/7	72.4	–	87.8	112.4
Neat LDPE	–	–	–	112.4

T_1, melting peak temperature of crystallization of EVA in quenching (peak 1); T_2, melting peak temperature of bundle-like crystallization of EVA (peak 2); T_3, melting peak temperature of folded-chain crystallization of EVA (peak 3); T_4, melting peak temperature of LDPE (peak 4).

EVA. Along with the further increase of LDPE in ratio, the depression in magnitude of such crystallization proportion is observed. It disappears when EVA/LDPE fraction riches to 3/7. Variable multiple melting reveals that more perfect crystal formed, competition of EVA between a nucleation effect on LDPE crystals and its partial miscibility in mixture may be responsible for such phenomenon.[20] Peak 1 changes to be a flatter and broader shape, and finally disappears in trace of neat LDPE, which represents the weakening of defective crystalline formed during intense under cooling condition. Data above imply that, the existence of VAc unit in EVA results in hindrance on crystallizability of both components in binary blends. More perfect crystallization could form along with the depressing of semicrystalline EVA fraction.

The highest endothermic peak 4 refers to the primary crystal melting of LDPE component. LDPE also has a wide short polyethylene chain branches distribution.[36] This leads to a continuous endothermic shoulder started at about 87.9°C, apparently lower than the primary melting peak at T_4 in its DSC curve. Such shoulder is close to the primary folded-chain crystallites melting of EVA component at T_3. After blending, overlapping endothermic peaks imply the existence of similar crystallizability of chain sequences distribution in both EVA and LDPE. Similar multiple melting has also been studied in other mixture systems. Melting peak 4 drops from 112.4°C to 109.8°C as the introduction of EVA component. Based on the characterization from Paul,[16] changes in multiple melting above clarifies some extent of crystalline phase miscibility in EVA/LDPE blend.

Evaluation of equilibrium melting temperature

T_m depresses significantly for a miscible blend. However, the melting temperature of a polymer is affected not only by the thermodynamic factors but also by the morphological factors.[37] Miscibility between polymer pair could be also indicated by the depression of the equilibrium melting temperature T_m^0, which could separate the morphological effect from thermodynamic effect in discussing the melting point depression as described by Flory–Huggins theory.[38] Equilibrium melting temperature T_m^0 implies the extrapolation to infinite thickness of lamellae, in such ideal situation, crystallization behavior and melting behavior of polymer reach dynamic balance.

Hoffman and Weeks proposed a relationship between the remarkable melting point T_m and the isothermal crystallization temperature T_c.

$$T_m = \eta T_c + (1 - \eta) T_m^0 \quad (5)$$

T_m^0 represents the equilibrium melting point. η is regarded as a measure of the stability, i.e. the lamellar thickness, of the crystals undergoing the melting process.[39] The T_m^0 can be obtained from the intersection of this line with the $T_m = T_c$ equation.

T_4 in Figure 2 refers to the highest melting peak temperature in LDPE component. Therefore, in order to reveal the interaction between LDPE and EVA, the T_m^0 of the comparative higher T_m component LDPE was studied. Blends involving variable LDPE fraction isothermally crystallized at different temperature from 30°C to 80°C for 10 min were investigated. Figure 3 shows the Hoffman–Weeks plots with extrapolation of the melting peaks temperature of blends. A linear correlation between T_m vs. T_c was obtained. T_m^0 of LDPE is 113.83°C via data extrapolation of linear fitting of peak temperature of T_4 at varying crystallization conditions. After having being mixed with EVA in blend, a slight depression is found. T_m^0 in blends drops apparently, to a lower scale, oscillating within 110.0°C and 110.9°C.

EVA is a kind of ethylene copolymer containing un-crystallizable polar groups VAc (wt % = 14%); LDPE has short branch chains linked to the backbone. The crystallizable units are all ethylene segments. Inter-molecular interaction may occur in the crystal regions. After blending EVA with LDPE, the primary crystalline melting of EVA and the apparent endothermic shoulder of LDPE has overlapped and exhibited only one endothermic peak, which proved the partial miscibility between them. This suggests that the tanglement of ethylene segments from both polymers have the same crystallizability, and led to some extent of co-crystallization during isothermal cooling. Such inter-molecular interaction also inhibited the primary crystallization of LDPE component apparently.

Effect of crystallization time

WAXD scan

Influences of time on WAXD are listed in Table III. The increase of time affects the lattice distance (*d-Val*) little. Lateral crystal size (L_{hkl}) grows to a larger degree as the time increases due to lamellar thickening. As for the quenched specimen, an intense under cooling condition supplies mobility to parts of chain segments to crystallize.

DSC analysis

Thermograms of EVA/LDPE = 7/3 blend crystallized at 70°C varying from 10 to 600 min are shown in Figure 4. Peak 2 does not form in specimens quenched defectively from the melting. Blends of other fractions quenched from melt also showed similar phenomenon. Crystal corresponding to the peak 2 only took place after the isothermal crystallization; this explains its absence in the quenched

TABLE III
WAXD Data of EVA/LDPE = 7/3 Blend Crystallized at 70°C for Different Times

Crystallization time/min	2θ (°)	Crystal plane	*d-Val* (Å)	L_{hkl} (Å)
Quenched	21.5	110	4.12	109.6
	23.9	200	3.72	97.0
	36.3	020	2.47	160.2
10	21.6	110	4.11	107.8
	23.9	200	3.72	77.4
	36.4	020	2.47	160.2
30	21.6	110	4.11	111.4
	23.9	200	3.72	80.4
	36.3	020	2.47	147.5
60	21.6	110	4.11	111.4
	23.9	200	3.72	81.8
	36.3	020	2.47	149.8
300	21.6	110	4.11	113.8
	23.9	200	3.72	85.6
	36.4	020	2.47	172.1
600	21.6	110	4.11	117.4
	23.9	200	3.72	84.8
	36.4	020	2.47	176.6

Parameter definition is the same as Table I.

sample.[40] Even the intense under cooling condition failed to form multiple crystallizations in EVA component. Chains involving VAc units were unable to arrange into lattice. Inter-molecular crystals were observed until sample isothermally crystallized for 10 min. Because all WAXD patterns in this work only observed the orthorhombic crystalline phase, and the multiple melting peak changes gradually along with the thermal history of sample, it is proved again that all the crystallizations referring to melting peaks 1, 2, 3, 4 are of the same crystalline phase.

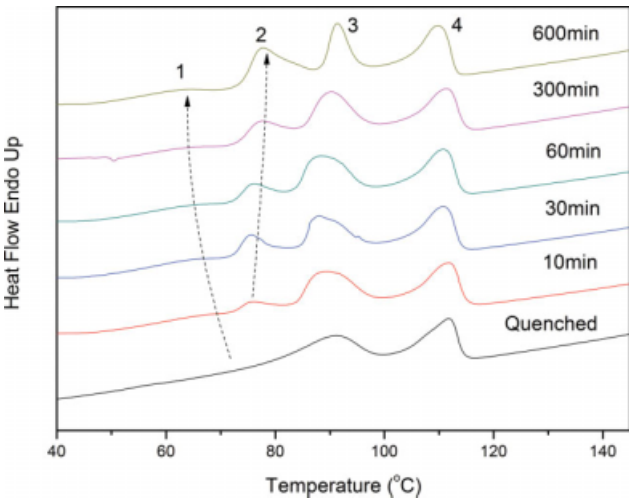

Figure 4 Endotherms of EVA/LDPE=7/3 blend crystallized at 70°C for different times. [Color figure can be viewed in the online issue, which is available at www.interscience.wiley.com.]

Table IV indicates that, prolongation of time had similar influence on crystallization as annealing has,[7] T_2 and T_1 ascend and depresses gradually as the passing of time, respectively. After crystallized isothermally for 600 min in 70°C water bath, peaks 2 and 3 increased in magnitude. Thermal trace shows sharper melting peaks for EVA component than earlier traces, which reveals a more perfect crystallites and comparative homogenous crystal lamellae thickness distribution in sample was obtained. On the contrary, a slight drop of T_4 is observed. The short chain branch sequences in EVA made the LLDPE chain in blend even more difficult to penetrate into inter-spherulitic regions after 600 min crystallization. Comparative similar short ethylene sequences distribution in both components might also result in co-crystallization and inter-molecular interaction. Similar co-crystallization in m-LLDPE/EVA blends has been verified by Wu et al.[10]

Crystallinity evaluation

Crystallinity of all blends with different EVA/LDPE ratios (10/0, 7/3, 5/5, 3/7, 0/10) was obtained from DSC and WAXD characterization, respectively. Figure 5 contrasts the X_c evaluation via both measurements in columnar section plots. In the calculation via DSC, it is accepted that the error in the experimentally determined enthalpies could not be negligible in view of baseline choosing. And it is apparent in Figure 2, the LDPE melting peak overlaps with part of EVA. An attempt to define the melting enthalpy of each components turns out to be difficult. In this work, crystallinity represents the entire percentage of ethylene chain sequences crystallized during experiment in both two components. Both groups of data grow to a higher degree along with the elongation of time. The upwards shifting trend of X_c attained from WAXD is at least 15% higher than results from DSC analysis, the growing tendency is also more obvious. The changing of blends fraction leads to larger influence on crystallinity than the time factor does. X_c grows much more

TABLE IV
Melting Peak Temperature of EVA/LDPE = 7/3 Blend Crystallized at 80°C for 10 min

Crystallization time	T_1	T_2	T_3	T_4
Quenched	–	–	90.6	111.8
10 min	65.6	75.9	89.2	111.7
30 min	64.4	75.6	88.0	110.7
60 min	63.4	76.2	88.4	110.7
300 min	63.1	77.8	90.2	111.4
600 min	61.9	77.9	91.4	109.7

Parameter definition is the same as Table II.

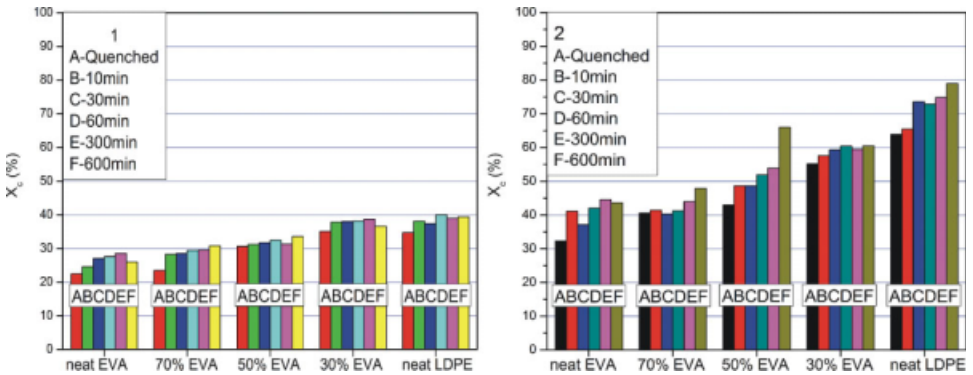

Figure 5 Relationship between X_c (1-DSC, 2-WAXD) and time of all samples at 70°C. [Color figure can be viewed in the online issue, which is available at www.interscience.wiley.com.]

apparently as the depression of EVA in binary blend with moderate oscillations.

Different measurements for crystallinity evaluation have been discussed by Lima et al.[41] Such difference was explained as the normalization factor utilized for the integration of enthalpies in crystallinity determination in DSC analysis, while Mo and Zhang[42] proposed that such difference could be explained as the difference in reflection of crystal defect and interface structure of two means. Evaluation via WAXD is based on the electron density difference between the amorphous region and the crystal region, density of latter is larger than the former. And the crystallinity is the corresponding reciprocal space intensity integral calculation of diffraction peaks and the amorphous region. The evaluation result includes both the contribution of crystal and amorphous region. The crystallinity calculation via DSC is based on heat flow integration. That is, the ratio of real endothermic enthalpy of specified sample against the energy of 100% crystallized polymer in ideal condition. The crystal region melting and some other enthalpy recovery by mobilization of minor rigid amorphous fraction in polymer all contribute to the value of X_c (%).

Effect of crystallization temperature

Figure 6 illustrates the development of crystallization behavior in blend EVA/LDPE = 7/3 with varying temperatures. Multiple melting is changing as a function of temperature. While sample being cooled from melt at 30°C, only the peak 3 referring to intramolecular folded chain crystal exists. Polymer chain segments involving VAc units were excluded from primary crystalline at this temperature, unable to arrange into lattice. This condition could not provide enough mobility for such chain segments to form inter-molecular crystallites at the interface of folded chain crystalline. Completion of secondary crystallization is perceptible when the temperature ascends. Endothermic peak of the melting behavior of intermolecular secondary crystallization (peak 2) keeps slightly higher than the crystallization temperature; besides, it shifts to a higher position monotonously. Peak shape changes to be sharper as the temperature increases.

Wang et al.'s[26] research in phase structure of EVA also found that, samples with different thermal history show changes in positions of multiple melting peaks, so as in the magnitude aspect. For EVA, VAc units are randomly introduced into the ethylene chains; they separated chains into crystalline ethylene sequences with different crystallizability. Higher crystallization temperature increases the mobility of chain segments while forming mobile secondary crystallization. The upwards shifting peak 2 temperature clarifies the completion process of secondary crystallization. Trace of blend crystallized at 80°C shows the sharpest peak shape at T_2, T_3, which means narrow lamellae thickness distribution of

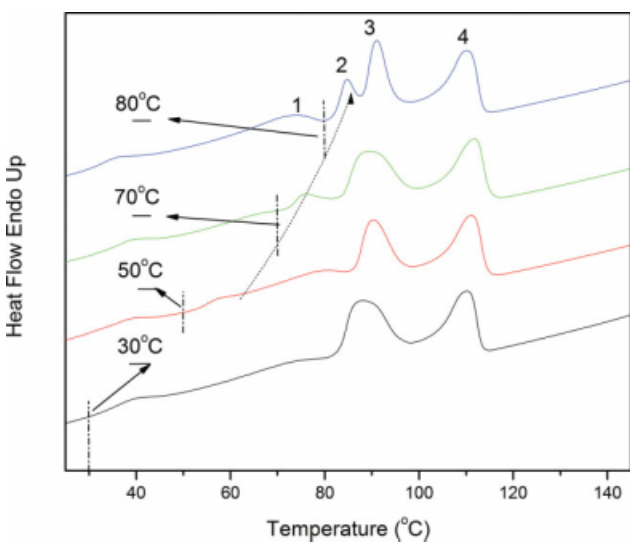

Figure 6 Endotherms of EVA/LDPE = 7/3 blend crystallized in different temperatures for 10 min. [Color figure can be viewed in the online issue, which is available at www.interscience.wiley.com.]

TABLE V
WAXD Data of EVA/LDPE = 7/3 Blend Crystallized in Different Temperatures for 10 min

Crystallization temperature (°C)	2θ (°)	Crystal plane	*d-Val* (Å)	L_{hkl} (Å)
30	21.6	110	4.11	110.9
	23.9	200	3.73	79.1
	36.4	020	2.47	168.9
50	21.6	110	4.11	104.5
	23.9	200	3.72	75.2
	36.4	020	2.47	147.5
70	21.6	110	4.11	110.9
	23.9	200	3.72	79.1
	36.4	020	2.47	168.9
80	21.6	110	4.11	115.2
	23.9	200	3.72	82.0
	36.4	020	2.47	140.8

Parameter definition is the same as for Table I.

crystalline in EVA component. The melting peak of LDPE does not fluctuate with temperature; such variable cannot affect its crystallization as it does to the peak 2.

WAXD data of sample crystallized at different temperatures in Table V exhibit a tendency consisted well with observation in DSC. No other crystalline phase formed or phase transition existed but only a unique orthorhombic phase existed in changing of crystallization temperature. Lattice distance (*d-Val*) of crystal plane keeps still. L_{hkl} rises with moderate fluctuation; higher crystallization temperature promotes the growth of lamellae. Lateral crystal size of (110) plane rises from about 110.9 Å to 115.2 Å. The overall crystallinity of blend does not change obviously along with the variation of temperature.

CONCLUSION

DSC results revealed that multiple melting depended on chain sequence distribution as function of the component ratio, crystallization temperature, and crystallization time. The primary folded-chain intra-molecular crystal of EVA component appeared at about 90°C was similar to the endothermic shoulder of LDPE. This clarified the approximate crystallizable ethylene sequence distribution in both components. The overlap of endothermic peaks of two components and drop of equilibrium melting temperature of LDPE extrapolated from Hoffman–Weeks plots clarified the partial miscibility in crystalline region, which was probably due to the intermolecular interaction or co-crystallization. WAXD parameters showed that both polymers had the identical orthorhombic crystalline phase structure, and the above-mentioned factors could not affect its predominant existence. The increase of LDPE fraction induced the growth in lateral crystal size and the decrease in lattice distance. Moderate extension of crystallization time and increase of crystallization temperature resulted in apparent upward shift of bundle-like crystal melting peak in EVA component and growth of lateral crystal size, which clarified the completion of secondary crystallization. Overall crystallinity of blend evaluated by DSC and WAXD grew higher with the reducing of EVA in ratio, as well as the increase of crystallization time. Influence of the mixture fraction on crystallinity was more remarkable than that of the crystallization time. Changing crystallization temperature did not affect the crystallinity apparently as the two former variables. Crystallinity evaluated from WAXD was at least 15% higher than the results from DSC. This could mostly be attributed to the difference in reflection of crystal defect and interface structure of two means.

References

1. Na, B.; Wang, Y.; Du, R. N.; Fu, Q.; Men, Y. F. J Polym Sci Part B: Polym Phys 2004, 42, 1831.
2. Khonakdar, H. A.; Jafari, S. H.; Yavari, A. Polym Bull 2005, 54, 75.
3. Wang, Z. G.; Hsiao, B. S.; Lopez, J.; Armistead, J. P. J Polym Res 1999, 6, 167.
4. Marie, E.; Chevalier, Y.; Eydoux, F.; Germanaud, L.; Flores, P. J Colloid Interface Sci 2005, 290, 406.
5. Maity, M.; Khatua, B. B.; Das, C. K. Polym Degrad Stab 2000, 70, 263.
6. Yao, D.; Li, R. H.; Nagarajan, P. Polym Eng Sci 2006, 46, 1223.
7. Huskic, M. J Appl Polym Sci 1996, 60, 1741.
8. Fonseca, C.; Ania, F. J Polym Sci Part B: Polym Phys 2001, 40, 913.
9. Okui, N.; Kawai, T. Die Macromol Chem 1971, 154, 161.
10. Wu, T.; Li, Y.; Zhang, D. L.; Liao, S. Q.; Tan, H. M. J Appl Polym Sci 2004, 91, 905.
11. Xu, H.; Kong, H.; Tang, Z. Polym Mater Sci Eng 2000, 16, 165.
12. Moly, K.; Bhagawan, S. S.; Groeninckx, G.; Thomas, S. J Appl Polym Sci 2006, 100, 4526.
13. Moly, K. A.; Radusch, H. J.; Androsh, R.; Bhagawan, S. S.; Thomas, S. Eur Polym J 2005, 41, 1410.
14. Russell, K. E.; Hunter, B. K.; Heyding, R. D. Polymer 1997, 38, 1409.
15. Uehara, H.; Nakae, M.; Kanamoto, T. Polymer 1998, 36, 6127.
16. Paul, D. R.; Bucknall, C. B. Polym. Blend; John Wiley & Sons Inc.: New York, 2004; Vol. 1.
17. Yoon, J. S.; Oh, S. H.; Kim, M. N. Polymer 1998, 39, 2479.
18. Yoon, J. S.; Oh, S. H.; Kim, M. N.; Chin, I. J.; Kim, Y. H. Polymer 1999, 40, 2303.
19. Kundu, R. P.; Tripathy, D. K. KGK-Kautschuk und Gummi Kunstst 1996, 49, 666.
20. Li, C. X.; Kong, Q. S.; Zhao, J.; Zhao, D. L.; Fan, Q. R.; Xia, Y. Z. Mater Lett 2004, 58, 3613.
21. Li, C. X.; Zhao, J.; Zhao, D. L. J Polym Res 2004, 11, 323.
22. Suryanarayana, C.; Grant, N. M. X-Ray Diffraction: A Practical Approach; Plenum Press: New York, 1998.
23. Zipper, P.; Janosi, A.; Geymayer, W. Polym Eng Sci 1996, 36, 467.
24. Brandrup, J.; Immergut, E. H. Polymer Handbook; John Wiley & Sons Inc.: New York, 1999.
25. Hu, W. G.; Eric, B. S. Macromolecules 2003, 36, 5144.
26. Wang, L. Y.; Fang, P. F.; Ye, C. H. J Polym Sci Part B: Polym Phys 2006, 44, 2864.

27. Nakamura, K.; Sawai, D.; Watanabe, Y. J Polym Sci Part B: Polym Phys 2003, 41, 1701.
28. Ma, W. Z.; Zhang, J.; Wang, X. L. J Macromol Sci Part B: Phys 2008, 41, 139.
29. Avila-Orta, C. A.; Medelln-Rodrguez, F. J.; Wang, Z.-G. Polymer 2003, 44, 1527.
30. Medellin-Rodriguez, F. J.; Phillips, P. J.; Lin, J. S. J Polym Sci Part B: Polym Phys 1997, 35, 1757.
31. Lammertink, R. G. H.; Hempenius, M. A.; Manners, I. Macromolecules 1998, 31, 795.
32. Righetti, M. C.; Tombari, E.; Di Lorenzo, M. L. Eur Polym J 2008, 44, 2659.
33. Chen, H.; Cebe, P. J Therm Anal Calorim 2007, 89, 417.
34. Minakov, A. A.; Mordvintsev, D. A.; Tol, R.; Schick, C. Thermochim Acta 2006, 442, 25.
35. Righetti, M. C.; Di Lorenzo, M. L.; Tombari, E.; Angiuli, M. J Phys Chem B 2008, 112, 4233.
36. He, M. J. Polymer Physics; Fudan University Press: Shanghai, 1990.
37. Nishi, T.; Wang, T. T. Macromolecules 1975, 8, 909.
38. Flory, P. J. Principles of Polymer Chemistry; Cornell University Press: Ithaca, New York, 1953.
39. Hoffman, J. D.; Weeks, J. J. J Chem Phys 1965, 42, 4301.
40. Di Lorenzo, M. L.; Righetti, M. C. Polymer 2008, 49, 1323.
41. Lima, M. F. S.; Vasconcellos, M. A. Z.; Samios, D. J Polym Sci Part B: Polym Phys 2002, 40, 896.
42. Mo, Z. S.; Zhang, H. F. Crystalline Polymer Structure and X-ray Diffraction; Science Press: Beijing, 2003.